Dalton Transactions

Variable Coordination of Carbazolyl-*bis*(tetrazole) Ligands in Lanthanide Chemistry

Journal:	*Dalton Transactions*
Manuscript ID	DT-ART-07-2018-002757.R1
Article Type:	Paper
Date Submitted by the Author:	03-Oct-2018
Complete List of Authors:	Gajecki, Leah; University of Victoria, Chemistry Berg, David; University of Victoria, Chemistry Hoenisch, Josh; University of Victoria, Chemistry Oliver, Allen; University of Notre Dame, Department of Chemistry and Biochemistry

Dalton Transactions

ARTICLE

Variable Coordination of Carbazolyl-*bis*(tetrazole) Ligands in Lanthanide Chemistry†

Leah Gajecki, [a] David J. Berg,*[a] Josh Hoenisch and Allen J. Oliver [b]

Received 00th January 20xx,
Accepted 00th January 20xx

DOI: 10.1039/x0xx00000x

www.rsc.org/

The synthesis of the protioligand 1,8-*bis*(2'-isopropyltetrazo-5'-yl)-3,6-di-tert-butylcarbazole, HCzT^{iPr} **2**, is described. The acid-base reaction of **2** with various Ln[N(SiMe$_3$)$_2$]$_3$ (Ln = Ce, Sm, Er, Yb, Y) precursors leads to products displaying a variety of different bonding modes for the CzT^{iPr-} ligand as revealed by X-ray crystallographic studies. The smaller lanthanides form Ln(CzT^{iPr})[N(SiMe$_3$)$_2$]$_2$ complexes (Ln = Er (**3**), Yb(**4**)) with a near planar, tridentate coordination mode for the CzT^{iPr-} ligand. In contrast, the larger lanthanides form Ln(CzT^{iPr})$_2$[N(SiMe$_3$)$_2$] complexes (Ln = Ce (**5**), Sm (**6**)) at room temperature that feature a sandwich structure with a highly distorted tridentate mode where tetrazole canting allows the metal to sit well out of the carbazole plane. Attempts to force additional CzT^{iPr-} ligands onto Er or Yb at elevated temperature results in isolation of trace siloxide complexes Ln(CzT^{iPr})$_2$(OSiMe$_3$) (Ln = Er (**3a**), Yb (**4a**)) that adopt a flat tridentate ligand bonding mode similar to **3** and **4**. Surprisingly, the high temperature reaction of **2** with Y[N(SiMe$_3$)$_2$]$_3$ affords Y(CzT^{iPr})$_3$, **7**, featuring two tridentate and one bidentate CzT^{iPr} ligands. Partial hydrolysis of **6** occurs over time to produce a hydroxo-bridged dimer that also features one bridging and one bidentate CzT^{iPr} ligand, Sm(κ^3-CzT^{iPr})(κ^3-μ-CzT^{iPr})(μ-OH)$_2$Sm(κ^3-CzT^{iPr})(κ^2-CzT^{iPr}), **6a**, further illustrating the remarkable coordinative flexibility of the CzT^{iPr} ligand system.

Introduction

Rigid multidentate donors have long been attractive as ligands because they offer control over the metal coordination environment.[1] This feature is especially useful in lanthanide chemistry where the predominantly ionic nature of the bonding and large ionic size allow a wide array of possible coordination modes. Limiting the coordinative options by imposing rigidity on the ligand framework is one way to introduce some predictability in the structural chemistry of these elements.

Previously we reported the chemistry of a carbazolyl-*bis*(oxazoline) ligand, Czx, with the lanthanides (Chart 1).[2,3] In all of the complexes we reported, the ligand coordinates in a planar, tridentate fashion through the anionic carbazolide and two neutral oxazoline nitrogens. This ligand allows formation of 5-coordinate *bis*(alkyl) erbium and ytterbium complexes that are stable to ligand redistribution even at elevated temperatures (Chart 1). However, the insertion activity of Ln(Czx)(CH$_2$SiMe$_3$)$_2$ (Ln = Er, Yb) was surprisingly limited towards alkenes (ethylene and styrene) and indeed, even when NMR spectroscopy clearly established the formation of the alkyl cations, [Ln(Czx)(CH$_2$SiMe$_3$)]$^+$[B(C$_6$F$_5$)$_4$]$^-$, insertions into the Ln-C bond proceeded at a remarkably slow rate.

To address some of the limitations of the Czx$^-$ ligand system and to expand the general family of tridentate chelates based on the anionic carbazolide core, we decided to prepare a related carbazolyl-*bis*(tetrazole) (CzT$^{iPr\,-}$, Chart 1) ligand and explore its reaction chemistry with the lanthanides.[4-8] This ligand is attractive for several reasons. First, it is less sterically encumbering than the Czx$^-$ ligand system because the lone substituent on the tetrazole ring is not adjacent to the binding nitrogen site. The incorporation of an isopropyl substituent one atom further removed from the coordinating nitrogen still provides some steric shielding that we hoped would prevent bridging interactions without placing as much bulk close to the metal centre. Second, the tetrazole rings make the CzT$^{iPr\,-}$ ligand far more electron rich than the Czx$^-$ system. This should stabilize higher oxidation states, such as Ce^{4+} and Yb^{3+}, in preference to the lower oxidation states of these metals. This provides an interesting comparison to the observation that trivalent Yb(Czx)(CH$_2$SiMe$_3$)$_2$ or Yb(Czx)Cl$_2$(THF) undergo *reduction* to *divalent* Yb(Czx)(PHAr)(THF)$_2$ on treatment with H$_2$PAr or LiPHAr, respectively, with oxidative phosphine coupling to produce ArPHPHAr.[3] Third, there are no structurally characterized lanthanide complexes containing neutral tetrazole ligands so the structural chemistry with this type of ligand is of interest.[9]

[a] Department of Chemistry, University of Victoria, PO Box 1700 Stn CSC, Victoria BC V8W 2Y2, Canada.
[b] Department of Chemistry & Biochemistry, University of Notre Dame, 251 Nieuwland Science Hall, Notre Dame, IN 46556, USA

† Dedicated to Professor Richard (Dick) Andersen on the occasion of his 75th birthday: an outstanding chemist, inspirational mentor and friend.

‡ Electronic Supplementary Information (ESI) available: crystallographic data for **2**, **3**, **3a**, **4**, **4a**, **5**, **6a** and **7** and NMR data for **1-7** (121 pages). See DOI: 10.1039/x0xx00000x

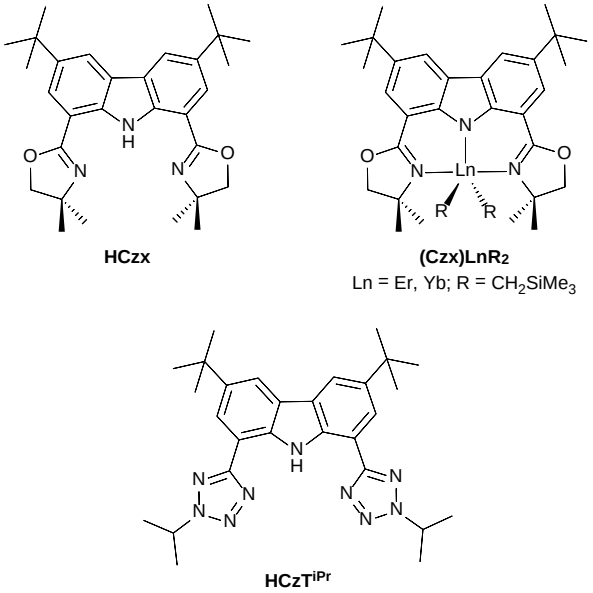

Chart 1 Carbazole-based pro-ligands and complexes discussed in this work.

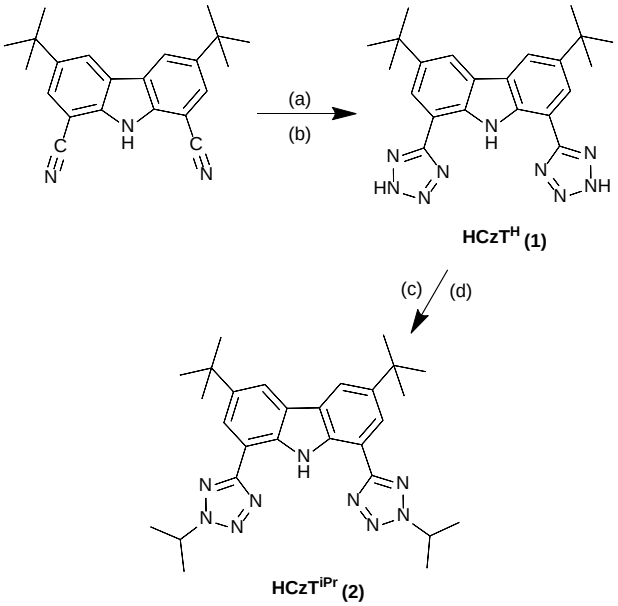

Scheme 1 Synthesis of pro-ligands $HCzT^{H}$ **(1)** and $HCzT^{iPr}$ **(2).** Conditions: (a) 2.5 equiv NaN_3, 0.2 equiv CAN, DMF, 140 °C, 48 h (b) EtOAc extraction, HCl, brine and water wash (c) 4 equiv K_2CO_3, DMF, 2.25 equiv iPrBr, 80 °C, 48h (d) EtOAc extraction, water wash.

In this contribution, we report the synthesis of the new ligand $HCzT^{iPr}$ and several of its lanthanide complexes. While the expected planar tridentate coordination mode is observed in some cases, the ligand can also adopt several other bonding modes. Structural types discussed below include a bridging mode through a second tetrazole nitrogen, an unusual distorted geometry in which the metal centre sits well out of the ligand plane and a bidentate chelate where one tetrazole is not coordinated. Unlike the Czx^{-} series, lanthanide complexes containing two and three CzT^{iPr-} ligands are observed.

Results and discussion

Synthesis

The unsubstituted parent ligand $HCzT^{H}$ **(1)** can be prepared in good yield from 1,8-dicyano-3,6-di-*tert*-butylcarbazole by the ceric ammonium nitrate catalysed cycloaddition of sodium azide (Scheme 1).[10] We have previously reported the synthesis of 1,8-dicyano-3,6-di-*tert*-butylcarbazole from carbazole and used this in reactions with amino alcohols to generate the HCzx family of ligands.[2] Alkylation of **1** can be carried out by deprotonation of the tetrazole ring with mild base (K_2CO_3) followed by addition of 2-bromopropane and heating at 80 °C for 2 days to afford $HCzT^{iPr}$ **(2)** in good yield (Scheme 1). The alkylation reaction also works well for other primary and secondary halides such as MeI and $PhCH_2Br$, but the resulting ligands are better suited for transition metal than lanthanide chemistry due to their smaller size.

Although deprotonation of the carbazole nitrogen in **2** is straightforward using NaH, previous work with Czx^{-} ligands revealed a tendency to form anionic *'ate'* complexes with salt inclusion during metathesis with lanthanide salts. The cleanest and most straightforward access to lanthanide complexes of CzT^{iPr-} is by direct protonolysis (acid-base reaction) of $Ln[N(SiMe_3)_2]_3$ with **2** (Scheme 2).

Reaction of 1 equivalent of **2** with $Ln[N(SiMe_3)_2]_3$ afforded the *mono*(ligand) complexes $Ln(CzT^{iPr})[N(SiMe_3)_2]_2$ (Ln = Er, **3**; Yb, **4**). The complexes were isolated in high purity as crystalline solvates from hot toluene. The simple ^1H NMR spectrum suggested that the complexes were monomeric with at least C_{2v} symmetry and this was confirmed by X-ray studies as discussed below.

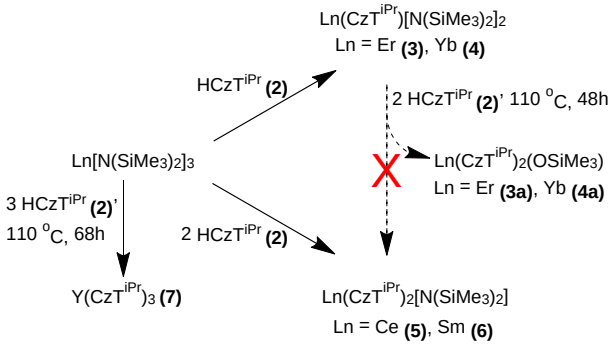

Scheme 2 Protonolysis of $Ln[N(SiMe_3)_2]_3$ with $HCzT^{iPr}$ **(2).** All reactions were carried out at room temperature unless otherwise specified.

Repeating the same reaction using 1 equivalent of **2** with the larger lanthanides $Ln[N(SiMe_3)_2]_3$ (Ln = Ce, Sm) afforded mixtures containing unreacted silylamide as well as a new product consistent with two CzT^{iPr} ligands and one $N(SiMe_3)_2$ group by ^1H NMR. Repeating these reactions with 2 equivalents of **2** cleanly produced $Ln(CzT^{iPr})_2[N(SiMe_3)_2]$ (Ln = Ce, **5**; Sm, **6**) in excellent yield (Scheme 2). The ^1H NMR spectra of **5** and **6**

showed equivalent CzT^{iPr-} ligands consistent with a high symmetry structure or a fluxional process in solution.

In light of the *bis*(CzT^{iPr}) structures, **5** and **6**, obtained with Ce and Sm, an attempt was made to force two ligands onto Er and Yb by carrying out the 2:1 ($HCzT^{iPr}$:$Ln[N(SiMe_3)_2]_3$) reaction at high temperature for an extended time (110 °C, 48 h). The main material isolated in this reaction consisted of **3** or **4** and unreacted $Ln[N(SiMe_3)_2]_3$, but during recrystallization, a small amount (< 5 %) of tiny needle-like crystals were isolated in both cases. These were examined by X-ray crystallography and found to indeed contain two CzT^{iPr-} ligands per metal centre but with a siloxide, rather than an intact silylamido ligand completing the coordination sphere: $Ln(CzT^{iPr})_2(OSiMe_3)$ (Ln = Er, **3a**; Yb, **4a**). We initially considered whether this could be an $^-NH(SiMe_3)$ ligand from degradation of the $^-N(SiMe_3)_2$ group but the geometry and bond lengths are more consistent with an $^-OSiMe_3$ unit (*vide infra*). The siloxide ligand could arise from hydrolysis of the $N(SiMe_3)_2$ ligand by trace moisture under prolonged heating or it could arise from trace oxo impurities in the starting $Ln[N(SiMe_3)_2]_3$. This reaction was reproducible, but the yield of this product was very small and prevented further characterization.

Similar hydrolysis was also observed for very small crystals of $Sm(CzT^{iPr})_2[N(SiMe_3)_2]$ **(6)** during the prolonged wait for access to synchrotron beam time. The fine yellow crystals of **6** were coated in Paratone oil and flame sealed in a glass ampoule, but over time these crystals slowly dissolved and very small orange crystals deposited. To our surprise, X-ray studies showed that the deposited crystals were a hydroxide-bridged dimer **(6a)** contained one CzT^{iPr-} ligand with a unique bridging tetrazole and another with a non-coordinated tetrazole unit within the same structure *(vide infra)*.

The isolation of degradation products **3a** and **4a** under forcing conditions prompted us to examine whether similar degradation products could be observed by ^1H NMR for a diamagnetic yttrium complex. The room temperature reaction of $Y[N(SiMe_3)_2]_3$ with 2 equivalents of $HCzT^{iPr}$ gave complex mixtures that could not be separated. However, the product that crystallized out of the reaction mixture on extended heating of $Y[N(SiMe_3)_2]_3$ with 2 equivalents of $HCzT^{iPr}$ showed a complicated ^1H NMR spectrum that contained no $N(SiMe_3)_2$ ligands! Elemental analysis and X-ray crystallography established this as the *tris*(ligand) complex, $Y(CzT^{iPr})_3$ **(7)**, containing both tridentate and bidentate CzT^{iPr} ligands (*vide infra*). Repeating the reaction in 3:1 stoichiometry resulted in cleaner product and higher yields. Throughout this work, no evidence of a *bis*(ligand) complex or silylamide degradation products were observed for **7**. This perhaps lends some credence to the idea that **3a** and **4a** arise from oxo containing impurities in the $Ln[N(SiMe_3)_2]_3$ (Ln = Er, Yb) starting materials rather than hydrolysis.

Structural Studies

The structure of the free ligand, $HCzT^{iPr}$ (**2**), was determined by X-ray diffraction. Crystallographic data is summarized in the ESI and the structure is illustrated in Figure 1. Unlike most of the complexes discussed below, **2** is close to planar (tetrazole = Tz cant angles relative to the carbazole plane: 6.8, 11.7°). This may well be to accommodate H-bonding between the carbazole NH and the adjacent tetrazole N. Also unlike the complexes discussed below, the *'inward'* pointing tetrazole N involved in the H-bonding is not the same position on each ring: one tetrazole uses the N adjacent to the isopropyl group while the other does not.

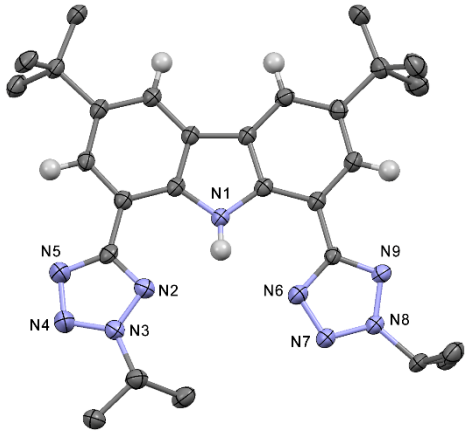

Figure 1 Thermal ellipsoid plot for **2** (50% probability). Isopropanol of crystallization and hydrogens on the t-Bu and i-Pr groups are not shown.

X-ray quality crystals of **3** and **4** as *bis*(toluene) solvates were grown from hot toluene solution. Crystallographic data are summarized in the ESI, selected bond distances and angles are collected in Table 1 and an ORTEP plot of **3** is shown in Figure 2. The complexes are isostructural and feature a distorted trigonal bipyramidal geometry with the carbazolide and silylamido N atoms occupying the equatorial sites and the tetrazole N in the axial positions. The Ln-N_{carb} distances of 2.368(3) and 2.347(2) Å for **3** and **4** respectively, are towards the long end of the range observed for other chelating carbazolide-lanthanide complexes after correction for differences in ionic radii and coordination number (range corrected to match Er^{3+} in 5 coordination: 2.235-2.400 Å; median: 2.302 Å).[2-6, 11] There are no neutral tetrazole complexes of the lanthanides, but the Ln-tetrazole distances here (**3**: 2.390(3), 2.401(3) Å; **4**: 2.392(2), 2.385(2) Å) are comparable to the Ln-oxazoline N distances in the Czx complexes previously reported by our group (range: 2.344-2.430; median: 2.363 Å) and the carbazole-*bis*(pyrazole) complexes reported by Hayes (range: 2.376-2.422; median: 2.412 Å). [2, 3, 5] The Ln-silylamide N distances are among the shortest such contacts for 5-coordinate Er and Yb silylamides reported (Er range: 2.220-2.318; median: 2.246 Å. Yb range: 2.161-2.380; median: 2.206 Å) suggesting that **3** and **4** are not exceptionally crowded.[12,13] Unlike the Czx ligands reported previously, the CzT ligand is not completely flat with the tetrazole rings canted about 8 and 16° out of the carbazole plane (in the same direction) in both structures. As a result, the Ln^{3+} ion lies slightly out of carbazole plane by the about 0.3 Å. This is a minor distortion in **3** and **4** but as the structures below illustrate, the CzT ligand is capable of much greater distortions from planarity.

Dalton Transactions

ARTICLE

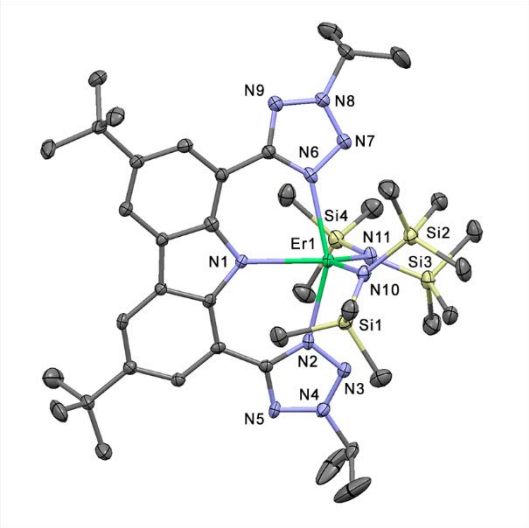

Figure 2 Thermal ellipsoid plot (50% probability) for **3**. Two toluenes of crystallization and all hydrogens omitted.

Table 1. Selected bond lengths and angles for $Ln(CzT^{iPr})[N(SiMe_3)_2]_2 \bullet 2\ C_7H_8$ (Ln = Er, **3**; Yb, **4**)[a]

	3 • 2 C_7H_8	**4 • 2 C_7H_8**
Ln-N_{carb}	2.368(3)	2.347(2)
Ln-N_{Tz1}	2.390(3)	2.392(2)
Ln-N_{Tz2}	2.401(3)	2.385(2)
Ln-N_{Sil1}	2.207(3)	2.120(2)
Ln-N_{Sil2}	2.226(3)	2.188(2)
Ln-carb plane[b]	0.34	0.33
N_{carb}-Ln-N_{Tz1}	77.20(10)	78.79(6)
N_{carb}-Ln-N_{Tz2}	78.68(10)	77.91(6)
N_{carb}-Ln-N_{Sil1}	113.63(11)	124.19(6)
N_{carb}-Ln-N_{Sil2}	123.98(10)	113.40(6)
N_{Tz1}-Ln-N_{Tz2}	153.46(10)	154.06(6)
N_{Tz1}-Ln-N_{Sil1}	102.44(11)	98.35(7)
N_{Tz1}-Ln-N_{Sil2}	84.83(11)	96.69(7)
N_{Tz2}-Ln-N_{Sil1}	97.23(11)	85.49(7)
N_{Tz2}-Ln-N_{Sil2}	99.74(11)	102.93(7)
N_{Sil1}-Ln-N_{Sil2}	121.40(11)	122.21(7)
Cant angle 1[c]	7.8	7.9
Cant angle 2[c]	16.3	16.5

[a] N_{carb}, N_{Tz1}, N_{Tz2}, N_{Sil1} and N_{Sil2} refer to the carbazolide nitrogen (N1 in both structures), tetrazole nitrogens (N2, N6 for **3**; N3, N7 for **4**) and silylamide nitrogens (N10 and N11 for both structures).
[b] distance of the Ln ion from the carbazole least squares plane.
[c] angle between the tetrazole and carbazole least squares plane

X-ray quality crystals of **5** containing 2.5 equivalents of toluene of solvation were grown by slow cooling a hot toluene solution. The structure confirmed the presence of two CzT^{iPr} ligands as indicated by ^{1}H NMR and elemental analysis. Crystallographic data are collected in Table S1 of the ESI, selected bond distances and angles are given in Table 2 and a structural plot is shown in Figure 3.

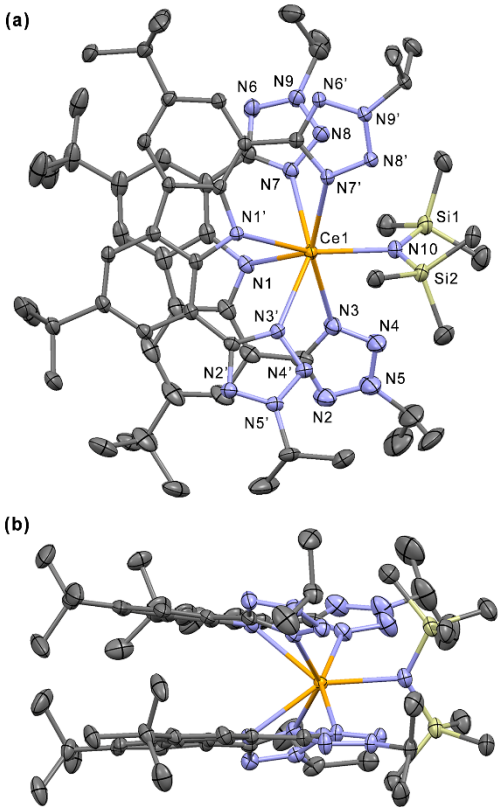

Figure 3 Thermal ellipsoid plot of **5** (50% probability): (a) top view (b) side view. Solvent of crystallization (2.5 equiv toluene) and hydrogens omitted.

Table 2. Selected bond lengths and angles for $Ce(CzT^{iPr})_2[N(SiMe_3)_2]$ • 2.5 C_7H_8 (**5 • 2.5 C_7H_8**), $Er(CzT^{iPr})_2(OSiMe_3)$ • 2.5 C_7H_8 (**3a • 2.5 C_7H_8**) and $Yb(CzT^{iPr})_2(OSiMe_3)$ • 2.33 C_7H_8 (**4a • 2.33 C_7H_8**)[a]

	5 • 2.5 C_7H_8	**3a • 2.5 C_7H_8**	**4a • 2.33 C_7H_8**
Ln-N_{carbA}	2.557(2)	2.374(3)	2.339(4)
Ln-N_{Tz1A}	2.680(2)	2.530(3)	2.491(5)
Ln-N_{Tz2A}	2.624(2)	2.465(3)	2.455(4)
Ln-N_{carbB}	2.566(2)	2.401(3)	2.361(4)
Ln-N_{Tz1B}	2.627(2)	2.451(3)	2.421(4)
Ln-N_{Tz2B}	2.703(2)	2.448(3)	2.434(4)
Ln-N_{Sil}	2.351(2)		
Ln-O		2.087(2)	2.061(4)
Ln-carb plane A[b]	1.483	1.281	1.262
Ln-carb plane B[b]	1.468	0.607	0.605
N_{carbA}-Ln-N_{Tz1A}	69.30(8)	72.99(9)	73.54(14)
N_{carbA}-Ln-N_{Tz2A}	69.72(7)	74.27(9)	74.74(14)
N_{carbA}-Ln-N_{carbB}	80.41(7)	155.73(9)	155.37(14)
N_{carbA}-Ln-N_{Tz1B}	84.79(7)	111.67(10)	110.42(15)
N_{carbA}-Ln-N_{Tz2B}	130.26(7)	83.71(9)	83.79(15)
N_{carbA}-Ln-N_{Sil}	136.00(8)		
N_{carbA}-Ln-O		103.28(9)	103.91(14)
N_{Tz1A}-Ln-N_{Tz2A}	116.82(8)	122.87(10)	123.64(15)
N_{Tz1A}-Ln-N_{carbB}	131.74(7)	87.27(9)	86.09(14)
N_{Tz1A}-Ln-N_{Tz1B}	70.51(7)	76.21(10)	75.33(15)
N_{Tz1A}-Ln-N_{Tz2B}	157.02(7)	77.32(10)	77.60(15)
N_{Tz1A}-Ln-N_{Sil}	78.56(7)		
N_{Tz1A}-Ln-O		156.29(9)	156.65(15)
N_{Tz2A}-Ln-N_{carbB}	84.26(7)	129.50(10)	129.27(13)
N_{Tz2A}-Ln-N_{Tz1B}	146.61(7)	74.25(10)	73.87(14)
N_{Tz2A}-Ln-N_{Tz2B}	68.77(7)	142.11(9)	141.99(14)
N_{Tz2A}-Ln-N_{Sil}	101.10(8)		
N_{Tz2A}-Ln-O		76.64(9)	76.27(15)
N_{carbB}-Ln-N_{Tz1B}	70.11(7)	75.86(10)	76.49(14)
N_{carbB}-Ln-N_{Tz2B}	69.41(7)	78.16(9)	78.31(13)
N_{carbB}-Ln-N_{Sil}	143.01(8)		
N_{carbB}-Ln-O		89.05(9)	89.25(14)
N_{Tz1B}-Ln-N_{Tz2B}	118.23(7)	143.46(10)	143.93(14)
N_{Tz1B}-Ln-N_{Sil}	112.27(8)		
N_{Tz1B}-Ln-O		125.38(10)	125.65(15)
N_{Tz2B}-Ln-N_{Sil}	78.47(8)		
N_{Tz2B}-Ln-O		78.99(9)	79.05(15)
Cant angle Tz_{1A}[c]	21.1	15.8	15.6
Cant angle Tz_{2A}[c]	22.0	17.9	17.9
Cant angle Tz_{1B}[c]	19.7	4.5	4.8
Cant angle Tz_{2B}[c]	10.3	3.0	2.8

[a] N_{carbA}, N_{Tz1A}, N_{Tz2A} refer to the carbazolide and tetrazole nitrogens of ligand A (N1, N3, N7 in **5** and **3a**; N1, N2 an N6 in **4a**) and N_{carbB}, N_{Tz1B}, N_{Tz2B} refer to the carbazolide and tetrazole nitrogens of ligand B (N1', N3', N7' in **5** and **3a**; N10, N11 and N15 in **4a**); N_{Sil} refers to the silylamide nitrogen (N10).
[b] distance of the Ln ion from the carbazole least squares plane.
[c] angle between the tetrazole and carbazole least squares plane

The immediately striking feature is that the carbazole planes of the two CzT^{iPr} ligands in **5** are almost coplanar (interplanar angle, 8.7°). The tetrazole rings of both CzT ligands are canted out of the carbazole plane of their ligand (CzT1: 10 and 20° and CzT2: 21 and 22°) so that the Ce^{3+} ion lies 1.48 and 1.47 Å out of the carbazole planes forming a sandwich structure. The two CzT ligands are not directly superimposed but are twisted with respect to one another by 28°, presumably to avoid interactions between the *i*-Pr substituents. The silylamido ligand sits in between the *i*-Pr substituents to complete the 7-coordinate geometry.

The Ce-N_{carb} distances in **5** of 2.557(2) and 2.566(2) Å are typical of other chelating carbazolide-lanthanide complexes after correction for differences in ionic radii and coordination number (range corrected to match Ce^{3+} in 7 coordination: 2.475-2.640 Å; median: 2.542 Å).[2-6, 11] The Ce-N_{Tz} distances range from 2.624(2)-2.703(2) Å which are long compared to the Ln-N distances in carbazole-oxazoline (corrected: 2.584-2.670 Å) and carbazole-pyrazole (2.616-2.662 Å) complexes.[2, 3, 5] The Ce-N distance for the silylamido group of 2.351(2)Å is the shortest observed in a 7-coordinate lanthanide silylamide structure after correction of the ionic radii to Ce^{3+} (range: 2.362-2.610; median: 2.434 Å).[11, 14]

Interestingly, the structure of $Y(CzT^{iPr})_3$, **7**, shares some structural features with **5**. Data collection parameters are summarized in ESI Table S2, selected bond distances and angles are given in Table 3 and a thermal ellipsoid plot of the structure is depicted in Figure 4. In this complex, two of the three CzT^{iPr} ligands are tridentate while the third is bidentate through the carbazolide and one tetrazole N. The tridentate CzT^{iPr} ligands, as in **5**, are close to coplanar at 14° and form a sandwich structure with the Y^{3+} ion 1.38 and 1.16 Å out of the carbazole planes. To accommodate the out of plane Y^{3+} ion, the tetrazoles in these two ligands are canted 17.9-21.0° out of the carbazole planes. The two coordinated nitrogens of the bidentate CzT^{iPr} ligand then occupy sites similar to the positioning of the silylamido ligand in **5**. The nonbonded tetrazole ring of the bidentate

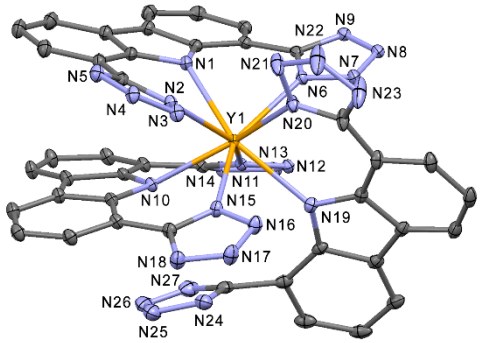

Figure 4 Thermal ellipsoid plot for **7** (50% probability). Disordered toluenes of solvation (0.87 equiv), hydrogens, t-Bu and i-Pr groups omitted for clarity.

ligand is twisted 61° out of the plane of its carbazole. All three Y-N_{carb} distances (2.378(2)-2.466(2) Å) are on the short end of the values predicted from literature complexes (corrected to Y^{3+}, 8-coordination, range: 2.425-2.590; median: 2.490 Å), as

are the Y-NTz distances (2.478(2)-2.544(2) Å) vs. predicted range: 2.534-2.620 Å).[2-6, 11]

Table 3. Selected bond lengths and angles for $Y(CzT^{iPr})_3$ • **0.87** C_7H_8 (**7** • **0.87** C_7H_8)[a]

Y1-N1$_{carbA}$	2.466(2)	Y1-N19$_{carbC}$	2.466(2)
Y1-N2$_{Tz1A}$	2.533(2)	Y1-N20$_{Tz1C}$	2.483(2)
Y1-N6$_{Tz2A}$	2.544(2)	Y1-carb plane A[b]	1.379
Y1-N10$_{carbB}$	2.378(2)	Y1-carb plane B[b]	1.157
Y1-N11$_{Tz1B}$	2.478(2)	Y1-carb plane C[b]	0.194
Y1-N15$_{Tz2B}$	2.488(2)		
N1-Y1-N2	71.71(6)	N10-Y1-N11	74.00(6)
N1-Y1-N6	70.43(6)	N10-Y1-N15	73.70(6)
N1-Y1-N10	80.98(6)	N10-Y1-N19	111.71(6)
N1-Y1-N11	80.06(6)	N10-Y1-N20	147.31(6)
N1-Y1-N15	136.53(6)	N11-Y1-N15	123.93(6)
N1-Y1-N19	149.67(6)	N11-Y1-N19	77.56(6)
N1-Y1-N20	106.07(6)	N11-Y1-N20	138.26(6)
N2-Y1-N6	118.49(6)	N15-Y1-N19	73.62(6)
N2-Y1-N10	78.61(6)	N15-Y1-N20	80.26(6)
N2-Y1-N11	143.20(6)	N19-Y1-N20	78.50(6)
N2-Y1-N15	69.07(6)	Cant angle Tz_{1A}[c]	17.9
N2-Y1-N19	136.41(6)	Cant angle Tz_{2A}[c]	21.0
N2-Y1-N20	73.80(6)	Cant angle Tz_{1B}[c]	20.9
N6-Y1-N10	137.82(6)	Cant angle Tz_{2B}[c]	18.5
N6-Y1-N11	71.07(5)	Cant angle Tz_{1C}[c]	15.5
N6-Y1-N15	147.11(6)	**Cant angle Tz_{2C}**[c]	**61.0**[d]
N6-Y1-N19	83.04(6)		
N6-Y1-N20	72.50(6)		

[a] N_{carbA}, N_{Tz1A}, N_{Tz2A} refer to the carbazolide and tetrazole nitrogens of ligand A; ligands B and C are designated in analogous fashion.
[b] distance of the Y ion from the carbazole least squares plane.
[c] angle between the tetrazole and carbazole least squares planes within a given ligand.
[d] non-coordinating tetrazole.

The silylamide degradation products **3a** and **4a** were isolated as minor crystalline by-products. These crystals were not representative of the bulk reaction products (**3** and **4**) but they do illustrate a different coordination environment for a *bis*(CzT^{iPr}) complex compared to that observed in **5**. Crystallographic data is summarized in ESI Table S2, selected bond lengths and angles are given in Table 2 and a thermal ellipsoid plot of **4a** is shown in Figure 5. While not isostructural, the structure of **3a** is effectively identical with that of **4a**. Unlike the nearly parallel arrangement of the two CzT^{iPr} ligands in **5** (and the tridentate CzT^{iPr} ligands in **7**), the two CzT^{iPr} ligands in **3a** and **4a** are nearly perpendicular to one another (81° in both). The geometry in **4a** (and **3a**) is best described as monocapped octahedral with the $OSiMe_3$ group capping a distorted octahedron comprised of the two nearly perpendicular CzT^{iPr} ligands. The tetrazole rings of one CzT^{iPr} ligand are canted significantly more than in the other (15.6-17.9° vs. 2.8-4.8°) and the Ln^{3+} ion lies further out of the carbazole plane of that ligand (1.262-1.283 Å vs. 0.605-0.607 Å). This distortion is presumably necessary to allow space for the capping $OSiMe_3$ group. Both the Ln-N_{carb} and Ln-N_{Tz} distances observed here are within the ranges predicted from literature values. The Ln-O distances and Ln-O-Si angles observed in **3a** and **4a** are also typical of other 7-coordinate lanthanide siloxides.[15]

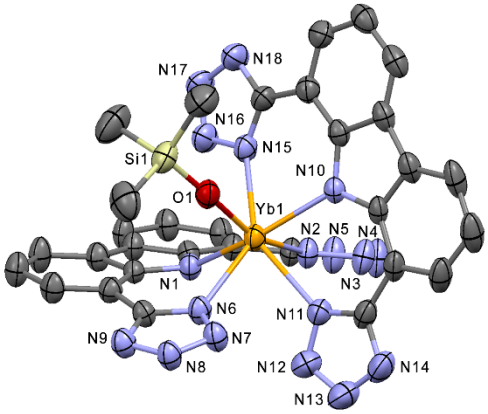

Figure 5 Thermal ellipsoid plot (50% probability) of **4a**. Toluenes of solvation (2.5 equiv), hydrogens, t-Bu and i-Pr groups omitted for clarity.

X-ray data were collected at the Advanced Light Source synchrotron facility at Lawrence Berkeley Laboratory on very small crystals of the partial hydrolysis product **6a** derived from $Sm(CzT^{iPr})_2[N(SiMe_3)_2]$, **6**. Crystallographic parameters are collected in ESI Table S2, selected bond distances and angles are given in Table 4 and a thermal ellipsoid plot of **6a** is shown in Figure 6. The structure of **6a** contains a bridging hydroxide in place of the silylamide ligand in **6** suggesting it arises from hydrolysis by trace water. The two Sm centers in **6a** are held together by two bridging hydroxides and one bridging tetrazole. The bridging tetrazole is bonded in the usual tridentate fashion to its own Sm but forms an additional bridge to the second Sm through the adjacent nitrogen (β to the tetrazole C). This type of bridging is very rare for neutral tetrazoles with one example known for a tetrazole-bridged silver complex.[16] For the Sm receiving this additional bridging N (Sm2 in Figure 6), one CzT^{iPr} ligand is tridentate and the other is bidentate with one non-coordinating tetrazole, similar to that observed in **7** (Figure 4). Both of the CzT^{iPr} ligands are tridentate on Sm1. One bridging oxygen (O2A/B) and two of the coordinating tetrazole groups (Tz_{1B} and Tz_{2D}) are positionally disordered in this structure. It is a concerted disorder that results in one tetrazole being coordinated in bridging fashion opposite the bridging oxygen (Tz_{1B} opposite O2A, shown in Figure 6; Tz_{2D} opposite O2B, not shown). The uncoordinated tetrazole is located almost perpendicular to the plane it adopts when it is coordinated. The ratio of this disorder was initially refined and yielded values close to 2/3:1/3 occupancy. In the final model these occupancies were set equal to 2/3 and 1/3 for the major and

minor components, respectively. The overall geometry at each 8-coordinate Sm center is based on a distorted square antiprism.

The Sm-N_{carb} distances in **6a** are within the expected range (predicted for Sm^{3+}, 8-coordination, range: 2.485-2.650; median: 2.552 Å). The Sm-N_{Tz} distances are at the shorter end of the predicted range including that for the tetrazole also involved in the bridging interaction (range: 2.594-2.680; median: 2.613 Å). The Sm2-$N12_{Tz1B}$ distance for the tetrazole bridging through the β-N is longer at 2.711(12) Å. The bridging OH distances, Sm1-O1 and Sm2-O1, of 2.250(8) and 2.241(8) Å, are somewhat shorter than typical bridging hydroxides for 7- and 8-coordinate Sm^{3+} centers (range: 2.277-2.389; median: 2.317 Å), but the distances to the disordered bridging OH opposite the bridging tetrazole, while not as precisely determined, are significantly longer (2.342(10)-2.41(3) Å).[17]

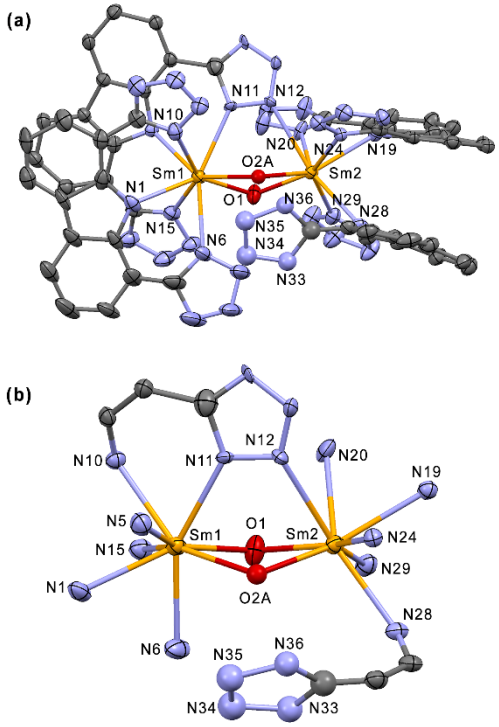

Figure 6 Thermal Ellipsoid plot for **6a** (30% probability): (a) Side view with t-Bu and i-Pr groups omitted for clarity (b) inner coordination sphere showing tetrazole rings disordered between bridging and non-coordinated positions *(see text).* Toluene (0.5 equiv) of solvation omitted for clarity.

Table 4. Selected bond lengths and angles for $[Sm(CzT^{iPr})_2]_2(\mu\text{-}OH)_2 \bullet 0.5\ C_7H_8$ (**6a • 0.5 C_7H_8**)[a]

Sm1-$N1_{carbA}$	2.539(9)	Sm2-$N19_{carbC}$	2.543(8)
Sm1-$N5_{Tz1A}$	2.597(11)	Sm2-$N20_{Tz1C}$	2.611(9)
Sm1-$N6_{Tz2A}$	2.559(11)	Sm2-$N24_{Tz2C}$	2.573(8)
Sm1-$N10_{carbB}$	2.522(8)	Sm2-$N28_{carbD}$	2.512(8)
Sm1-$N11_{Tz1B}$	**2.563(11)[e]**	Sm2-$N29_{Tz1D}$	2.531(10)
Sm1-$N15_{Tz2B}$	2.588(10)	**Sm2-$N12_{Tz1B}$**	**2.711(12)[e]**
Sm1-O1	2.250(8)	Sm2-O1	2.241(8)
Sm1-O2A	2.342(10)	Sm2-O2A	2.391(10)
Sm1-O2B	2.41(3)	Sm2-O2B	2.35(3)
Sm1-carb plane A[b]	1.248	Sm2-carb plane C[b]	1.390
Sm1-carb plane B[b]	1.454	Sm2-carb plane D[b]	1.306
Sm1-O1-Sm2	112.9(3)	Sm1-O2A-Sm2	106.9(4)
Sm1-O2B-Sm2	103.7(11)		
Cant angle Tz_{1A}[c]	16.6	Cant angle Tz_{1C}[c]	13.8
Cant angle Tz_{2A}[c]	9.3	Cant angle Tz_{2C}[c]	26.0
Cant angle Tz_{1B}[c]	**26.3[e]**	Cant angle Tz_{1D}[c]	17.4
Cant angle Tz_{2B}[c]	21.7	**Cant angle Tz_{2D}[c]**	**58.5[f]**
Carb A/B angle[d]	10.8	Carb C/D angle[d]	15.4

[a] N_{carbA}, N_{Tz1A}, N_{Tz2A} refer to the carbazole and tetrazole nitrogens of ligand A; ligands B-D are designated in analogous fashion.
[b] distance of the Sm ion from the carbazole least squares plane.
[c] angle between the tetrazole and carbazole least squares planes within a given ligand.
[d] angle between the carbazole planes on a given Sm center.
[e] this tetrazole bridges the two Sm centers when the disordered OH is in position O2A; Tz_{2D} bridges when the disordered OH is In position O2B (not shown here).

Experimental

All experiments were performed under an atmosphere of nitrogen on a vacuum line or in a glovebox (MBraun) at room temperature unless otherwise specified. All solvents and reagents were purchased from Aldrich Chemicals and used as received except for 3,6-di-*tert*-butylcarbazole, 1,8-dibromo-3,6-di-*tert*-butylcarbazole and 1,8-dicyano-3,6-di-*tert*-butylcarbazole, which were prepared as previously described.[2] $Ln[N(SiMe_3)_2]_3$ complexes were prepared according to literature methods.[18] NMR spectra were recorded in dmso-d_6, benzene-d_6, toluene-d_8 or THF-d_8 on a Bruker AMX 300, 360 or 500 MHz NMR spectrometer. Melting points were determined in sealed capillaries on a Gallenkamp MFB 600 030W instrument and are uncorrected. +ESI-MS data were collected on a Q-TOF II instrument by MicroMass. Elemental analyses (C, H, N) were carried out by Canadian Microanalytical Ltd., Delta, B.C. Most analytical samples were recrystallized from toluene-hexane mixtures and the microcrystalline solids obtained were exposed to vacuum for several hours prior to sealing in a glass ampoule under partial vacuum. As a result, the elemental analysis obtained does not necessarily match the solvation found in X-

ray samples. The calculated analyses reported are the best fit to the observed values based on the solvents of crystallization used.

Ligand Synthesis

1,8-Bis(2'-H-tetrazo-5'-yl)-3,6-di-tert-butylcarbazole, HCzT^{H} 1 1,8-dicyano-3,6-di-*tert*-butylcarbazole (4.14 g, 13.1 mmol) was dissolved in DMF (60 mL) in a round bottom flask and the solution placed under a nitrogen atmosphere. Solid ceric ammonium nitrate (1.39 g, 2.54 mmol) was added and the solution was heated 140 °C. Solid NaN_3 (2.11 g, 32.5 mmol) was added to the hot solution and the colour changed from light orange to dark brown. The suspension was refluxed for 48 h, cooled to room temperature and extracted with ethyl acetate (2 x 150 mL) in air. The combined organic layers were washed with 1M HCl (2 x 100 mL), brine (2 x 100 mL) and finally water (2 x 100 mL). The organic phase was then dried over anhydrous $MgSO_4$, filtered and the filtrate taken to dryness under reduced pressure to give a light yellow-brown crude product. Washing with a minimum of ethyl acetate produced pure **1** as a light yellow powder. The product was isolated as a *bis*(ethyl acetate) solvate. Yield: 4.78 (88%). Mp. dec. 240 °C. ^{1}H NMR (dmso-d_6, 300 MHz): δ 17.2 (br s, 2H, 2'-NH), 11.75 (s, 1H, N*H*), 8.63 (br s, 2H, 4,5-aryl*H*), 8.33 (br s, 2H, 2,7-aryl*H*), 4.01 (q, 4H, ethyl acetate CH_2), 1.97 (s, 6H, ethyl acetate CH_3), 1.50 (s, 18H, CCH_3), 1,16 (t, 6H, ethyl acetate CH_3). ^{13}C{^{1}H}(dmso-d_6, 75.5MHz): δ 170.32 (*C5'*), 142.82 (*C3/6*), 135.29 (*C9a/d*), 123.79 (*C9b/c*), 122.35 (*C4/5*), 120.81 (*C2/7*), 105.88 (*C1/8*), 59.76 (ethyl acetate OCH_2), 34.92 ($C(CH_3)_3$), 31.78 ($C(CH_3)_3$), 20.74 (ethyl acetate C(O)CH_3), 14.08 (ethyl acetate CH_2CH_3).

1,8-Bis(2'-isopropyltetrazo-5'-yl)-3,6-di-tert-butylcarbazole, HCzT^{iPr} 2 A Schlenk tube was charged with finely ground K_2CO_3 (0.668 g, 4.83 mmol) and DMF (30 mL) and the suspension placed under a nitrogen atmosphere. In a separate flask, **1** (0.500 g, 1.19 mmol) was dissolved in 30 mL DMF and this solution was added to the Schlenk tube. 2-Bromopropane (0.25 mL, 2.66 mmol) was added to the reaction mixture by syringe and the vigorously stirred solution was heated at 80 °C for 48 h. On cooling, the yellow solution was diluted with ethyl acetate (200 mL) in air and washed repeatedly (4 x 300 mL) water to remove DMF. The ethyl acetate phase was dried over anhydrous $MgSO_4$, filtered and the filtrate taken to dryness under reduced pressure. The crude yellow powder was recrystallized from hot isopropanol to yield pure **2** as a white powder. Yield: 0.494 g (83%). Mp. 204-206 °C. ^{1}H NMR (dmso-d_6, 300 MHz): δ 11.43 (br s, 1H, N*H*), 8.58 (d, $^4J_{HH}$ = 1.5 Hz, 2H, 4,5-aryl*H*), 8.29 (d, $^4J_{HH}$ = 1.5 Hz, 2H, 2,7-aryl*H*), 5.32 (septet, $^3J_{HH}$ = 7.5 Hz, 2H, 2'-NC*H*), 1.76 (d, $^3J_{HH}$ = 7.5 Hz, 12H, 2'-NCH(CH_3)$_2$), 1.49 (s, 18H, CCH_3). ^{13}C{^{1}H}(dmso-d_6, 75.5 MHz): δ 163.05 (*C5'*), 142.46 (*C3/6*), 135.12 (*C9a/d*), 123.76 (*C9b/c*), 120.94 (*C2/7*), 120.00 (*C4/5*), 108.82 (*C1/8*), 56.64 (2'-N*C*H), 34.66 (*C*$(CH_3)_3$), 31.79 (C(*C*H_3)$_3$), 21.95 (2'-NCH(*C*H_3)$_2$). +ESI-MS: *m/z* 522.306 (M^+ + Na, calcd. 522.307).

Er(CzT^{iPr})[N(SiMe$_3$)$_2$]$_2$ 3 In the glovebox, one equiv of HCzT^{iPr}, **2**, (0.100 g, 0.200 mmol) dissolved in toluene was added to a solution of one equiv of Er[N(SiMe$_3$)$_2$]$_3$ (0.130 g, 0.200 mmol) dissolved in toluene. The resulting yellow solution was stirred overnight and slowly turned orange in colour. The solvent was removed under reduced pressure and the crude product was washed with hexanes to yield an orange powder. Recrystallization of crude powder in hot toluene afforded yellow crystals of **3**. Yield: 0.191 g (97%). Mp. 240-234˚C. ^{1}H NMR (300 MHz, benzene-d_6, 298K): δ 52.03 (s, 2H, $\upsilon_{1/2}$ = 60 Hz, aryl*H*), 40.66 (s, 2H, $\upsilon_{1/2}$ = 60 Hz, aryl*H*), 34.37 (s, 12H, $\upsilon_{1/2}$ = 27 Hz, CH(CH_3)$_2$), 4.89 (s, 18H, $\upsilon_{1/2}$ = 10 Hz, C(CH_3)$_3$), 4.58 (s, 2H, $\upsilon_{1/2}$ = 16 Hz, C*H*$(CH_3)_2$), -10.53 (s, 36H, $\upsilon_{1/2}$ = 220 Hz, Si(CH_3)$_3$). Anal. Calcd. for $C_{40}H_{72}N_{11}Si_4Er$: C 48.69, H 7.35, N 15.62; found: C 53.48, H 7.82, N 13.76. Anal calcd. for the solvate **3** • 1.5 toluene: C 53.92, H 7.53, N 13.70. The analytical sample was exposed to vacuum after recrystallization presumably resulting in partial solvent loss.

Yb(CzT^{iPr})[N(SiMe$_3$)$_2$]$_2$ 4 This complex was prepared by an analogous procedure to **3** using 0.200 g (0.400 mmol) **2** and 0.261 g (0.400 mmol) Yb[N(SiMe$_3$)$_2$]$_3$. Recrystallization of the crude orange powder from hot toluene afforded yellow crystals of **4**. Yield: 0.325 g (82%). Mp. 241-244˚C. ^{1}H NMR (300 MHz, benzene-d_6, 298K): δ 42.57 (s, 2H, $\upsilon_{1/2}$ = 35 Hz, aryl*H*), 29.34 (s, 2H, $\upsilon_{1/2}$ = 24 Hz, aryl*H*), 27.62 (s, 12H, $\upsilon_{1/2}$ = 20 Hz, CH(CH_3)$_2$), 2.02 (s, 18H, $\upsilon_{1/2}$ = 7 Hz, C(CH_3)$_3$), -0.89 (s, 2H, $\upsilon_{1/2}$ = 9 Hz, C*H*$(CH_3)_2$), -12.22 (s, 36H, $\upsilon_{1/2}$ = 95 Hz, Si(CH_3)$_3$). Anal. Calcd. for $C_{40}H_{72}N_{11}Si_4Yb \bullet C_7H_8$: C 52.05, H 7.43, N 14.21; found: C 49.06, H 6.98, N 13.75. The X-ray structure contains 2 equivalents of toluene but partial loss of solvent is likely under vacuum. The best compromise is 1 equiv of toluene of solvation, although in this case, the C % found would be quite low.

Ce(CzT^{iPr})$_2$[N(SiMe$_3$)$_2$] 5 In the glovebox, two equivs of HCzT^{iPr}, **2**, (0.500 g, 1.00 mmol) dissolved in toluene was added to a solution of one equiv of Ce[N(SiMe$_3$)$_2$]$_3$ (0.310 g, 0.500 mmol) dissolved in toluene. The resulting yellow solution was stirred overnight and slowly turned orange in colour. The solvent was removed under reduced pressure and the crude product was washed with hexanes to yield an orange powder. Recrystallization of the crude powder in hot toluene-hexane afforded fine yellow crystals of **5**. Yield: 0.632 g (98%). Mp. 290˚C (dec). ^{1}H NMR (360 MHz, toluene-d_8, 353K): δ 13.34 (s, 4H, $\upsilon_{1/2}$ = 65 Hz, aryl*H*), 8.88 (s, 4H, $\upsilon_{1/2}$ = 136 Hz, aryl*H*), 3.12 (s, 40H, $\upsilon_{1/2}$ = 45 Hz, C(CH_3)$_3$ and C*H*$(CH_3)_2$), 0.06 (s, 18H, $\upsilon_{1/2}$ = 36 Hz, Si(CH_3)$_3$), -0.22 (s, 24H, $\upsilon_{1/2}$ = 60 Hz, CH(CH_3)$_2$). Anal. Calcd. for $C_{62}H_{90}CeN_{19}Si_2$: C 57.38, H 6.99, N 20.51; found: C 61.10, H 7.73, N 18.40. Anal calcd. for the solvate **5** • toluene • hexane: C 61.03, H 7.65, N 18.03.

Sm(CzT^{iPr})$_2$[N(SiMe$_3$)$_2$] 6 This complex was prepared by an analogous procedure to **5** using 0.200 g (0.400 mmol) **2** and 0.126 g (0.200 mmol) Sm[N(SiMe$_3$)$_2$]$_3$. Recrystallization of the crude yellow powder from hot toluene afforded yellow crystals of **6**. Yield: 0.288 g (91%). Mp. 312˚C (dec). ^{1}H NMR (360 MHz, benzene-d_6, 343K): δ 9.05 (s, 4H, $\upsilon_{1/2}$ = 40 Hz, aryl*H*), δ8.49 (s, 4H, $\upsilon_{1/2}$ = 50 Hz, aryl*H*), 4.70 (s, 2H, $\upsilon_{1/2}$ = 90 Hz, C*H*$(CH_3)_2$), 2.02 (s, 36H, $\upsilon_{1/2}$ = 25 Hz, C(C*H*)$_3$), 1.31 (s, 24H, $\upsilon_{1/2}$ = 55 Hz, CH(CH_3)$_2$), -0.81 (s, 18H, $\upsilon_{1/2}$ = 35 Hz, Si(CH_3)$_3$), -2.38 (s, 2H, $\upsilon_{1/2}$ = 120 Hz, C*H*$(CH_3)_2$). Anal. Calcd. for $C_{62}H_{90}SmN_{19}Si_2$: C 56.93, H 6.93, N 20.35; found: C 58.10, H 7.41, N 19.05. Anal calcd. for the solvate **6** • hexane: C 58.58, H 7.52, N 19.09. The analytical

sample was washed repeatedly with hexane and exposed to vacuum.

Y(CzT^{iPr})$_3$ 7 In the glovebox, three equivs of HCzT^{iPr}, **2**, (0.0250 g, 0.0500 mmol) dissolved in toluene was added to a solution of one equiv of Y[N(SiMe$_3$)$_2$]$_3$ (0.0095 g, 0.017 mmol) dissolved in toluene. The resulting yellow solution and a small magnetic stir bar were placed in a Kontes flask and sealed before removal from the glovebox. The flask was immersed in an oil bath at 110 °C and heated with stirring for 68h. The flask was returned to the glovebox and the solvent was removed under reduced pressure. The crude yellow powder was washed repeatedly with hexane and recrystallization from hot toluene to afford yellow crystals of **7**. Yield: 0.0241 g (91 %). Mp. 292 ˚C (dec). ^{1}H NMR (300 MHz, benzene-d$_6$): δ 8.55 (m, 2H, aryl*H*), 8.20 (m, 2H, aryl*H*), 8.10 (m, 2H, aryl*H*), 7.98 (m, 2H, aryl*H*), 7.90 (m, 2H, aryl*H*), 7.79 (m, 2H, aryl*H*), 4.26 (br m, 2H, C*H*(CH$_3$)$_2$), 4.15 (br m, 2H, C*H*(CH$_3$)$_2$), 3.27 (br m, 2H, C*H*(CH$_3$)$_2$), 1.50-1.68 (br overlapping s, 54H, C(C*H*$_3$)$_3$), 1.22 (br m, 6H, CH(C*H*$_3$)$_2$), 1.12 (br m, 3H, CH(C*H*$_3$)$_2$), 0.88-0.96 (br m, 18H, CH(C*H*$_3$)$_2$), 0.60 (br m, 9H, CH(C*H*$_3$)$_2$). Anal. Calcd. for $C_{84}H_{108}N_{27}Y$: C 63.66, H 6.87, N 23.86; found: C 62.80, H 6.26, N 22.55.

Crystallography

Crystals of **2** were grown by slow cooling a hot isopropanol solution. Crystals of **3**, **3a**, **4**, **4a**, **5** and **7** were grown from hot toluene solution by slow cooling. Crystals of **6** were coated in Paratone N oil but over several weeks these slowly dissolved and crystals of **6a** deposited. X-ray data for **2**, **3**, **3a**, **5** and **7** was collected on a Bruker APEX-II diffractometer (Mo Kα, λ = 0.71073 Å) using a combination of ω- and ϕ-scans of 0.5°.[19] X-ray data for **4**, **4a** and **6a** were collected on a Bruker PHOTON-100 CMOS diffractometer (λ_{synch} = 0.77490 Å for **4**, **4a** and 1.0332 Å for **6a**) using a combination of ω- and ϕ-scans of 0.5°. Data were corrected for absorption and polarization effects and analyzed for space group determination.[20] The structure was solved by dual-space methods and expanded routinely.[21] The model was refined by full-matrix least-squares analysis of F^2 against all reflections.[21, 22] All non-hydrogen atoms were refined with anisotropic atomic displacement parameters. Unless otherwise noted, hydrogen atoms were included in calculated positions. In most of these structures, the t-butyl and isopropyl groups displayed rotational disorder and in many cases the toluene of solvation was disordered. The appropriate disorder models were refined in each case.

In addition to the positional disorder noted for **6a** in the discussion, there is exaggerated motion in the peripheral groups. In general, disordered atoms were modelled with isotropic atomic displacement parameters for this structure. Additionally, the data were truncated at 0.90 Å, because, despite the utilization of the extra intensity of a synchrotron radiation source, there was poor diffraction at higher resolutions. Presumably, the high degree of disorder in the extremities of the complex is one cause for this decrease in intensity. Despite the lower than normal data resolution, the connectivity of the complex is unequivocal. Bond distances and angles for **6a** have high standard uncertainties, again, a result of the disorder and lower than normal data quality. These metrics are however, within acceptable limits. The CCDC deposition numbers for the structures described here are 1853581 (**2**), 1853585 (**3**), 1853586 (**3a**), 1853582 (**4**), 1853583 (**4a**), 1853587 (**5**), 1853584 (**6a**) and 1853588 (**7**).

Conclusions

The carbazole-*bis*(tetrazole) family of ligands is easily accessible and the parent ligand HCzT^H (**1**) is readily alkylated to form HCzT^{iPr} (**2**). The deprotonated form CzT^{iPr-} is a versatile ligand for lanthanide chemistry displaying a rich and varied coordination chemistry. As demonstrated here, this ligand appears equally capable of bonding through a close-to-planar tridentate mode (*e.g.* **3, 3a, 4, 4a**) or through a highly distorted tridentate mode where tetrazole canting allows the metal to sit well out of the carbazole plane favouring sandwich complexes (*e.g.* **5, 7**). Additionally we have shown that this ligand can also adopt a bidentate bonding mode (*e.g.* **6a, 7**) and that bridging interactions through a second tetrazole nitrogen are possible (*e.g.* **6a**). We anticipate this ligand system will continue to generate a wealth of unusual lanthanide and transition metal chemistry.

Conflicts of interest

There are no conflicts to declare.

Acknowledgements

DJB acknowledges the support of a NSERC Discovery Grant (Canada). Crystallographic data on **4**, **4a** and **6a** were collected at Beamline 11.3.1 at the Advanced Light Source (ALS), Lawrence Berkeley National Laboratory by AJO. The ALS is supported by the U.S. Dept. of Energy, Office of Energy Sciences, under contract DE-AC02-05CH11231.

Notes and references

1 *See for example:* N. Kazeminejad, D. Munzel, M. T. Gamer and P. W. Roesky, *Chem. Commun*. 2017, **53**, 1060 and references therein.
2 J. Zou, D. J. Berg, B. McDonald and A. Oliver, *Organometallics*, 2011, **30**, 4958.
3 J. Zou, D.J. Berg, A. Oliver and B. Twamley, *Organometallics*, 2013, **32**, 6532.
4 Related carbazole-*bis*(phosphinimine) lanthanide complexes: K. R. D. Johnson and P. G. Hayes, *Organometallics*, 2009, **28**, 6352; K. R. D. Johnson and P. G. Hayes, *Organometallics*, 2011, **30**, 58; K. R. D. Johnson and P. G. Hayes, *Organometallics*, 2013, **32**, 4046; K. R. D. Johnson and P. G. Hayes, *Inorg. Chim. Acta*, 2014, **422**, 209; K. R. D. Johnson and P. G. Hayes, *Dalton Trans.*, 2014, **43**, 2448; K. R. D. Johnson, B. L. Kamenz and P. G. Hayes, *Can. J. Chem.*, 2016, **94**, 330.

5 Related carbazole-*bis*(pyrazole) lanthanide complexes: K. R. D. Johnson and P. G. Hayes, *Organometallics*, 2014, **33**, 3005.
6 Related carbazole-*bis*(phosphine(lanthanide complexes: L. Wang, D. Cui, Z, Hou, W. Li and Y. Li, *Organometallics*, 2011, **30**, 760.
7 Related carbazole-*bis*(pyridine(ligands: M. S. Mudadu, A. N. Singh and R. P. Thummel, *J. Org. Chem.* 2008, **73**, 6513.
8 Related carbazole-*bis*(N-heterocyclic carbene) ligands: M. Moser, B. Wucher, D. Kunz and F. Rominger, *Organometallics*, 2007, **26**, 1024.
9 E. S. Andreiadis, D. Imbert, J. Pécault, R. Demadrille and M. Mazzanti, *Dalton Trans.* 2012, **41**, 1268.
10 S. Kumar, S. Dubey, N. Saxena, S. Kumar Awasthi, *Tet. Lett.*, 2014, **55**, 6034.
11 R. D. Shannon, *Acta Cryst. Sect. A*, 1976, **A32**, 751.
12 S. A. Scheutz, V. W. Day, J. L. Clark and J. A. Belot, *Inorg. Chem. Commun.* 2002, **5**, 706; S. A. Scheutz, C. M. Silvernail, C. D. Incarvito, A. L. Rheingold, J. L. Clark, V. W. Day and J. A. Belot, *Inorg. Chem.*, 2004, **43**, 6203; W. J. Evans, D. S. Lee, D. B. Rego, J. M. Perotti, S. A. Kozimor, E. K. Moore and J. W. Ziller, *J. Am. Chem. Soc.*, 2004, **126**, 14574; S. Jank, C. Guttenberger, H. Reddmann, J. Hanss and H.-D. Amberger, *Z. Anorg. Allg. Chem.*, 2006, **632**, 2429; P. L. Arnold, J.-C. Buffet, R. Blaudeck, S. Sujecki and C. Wilson, *Chem. Eur. J.*, 2009, **15**, 8241; M. Fang, T. E. Bates, S. E. Lorenz, D. S. Lee, D. B. Rego, J. W. Ziller, F. Furche and W. J. Evans, *Inorg. Chem.*, 2011, **50**, 1459; J. D. Rinehart, M. Fang, W. J. Evans and J. R. Long, *J. Am. Chem. Soc.* 2011, **133**, 14236; Q. Li, S. Zhou, S. Wang, X. Zhu, L. Zhang, Z. Feng, L. Guo, F. Wang and Y. Wei, *Dalton Trans.*, 2013, **42**, 2861; X. Gu, X. Zhu, Y. Wei, S. Wang, S. Zhou, G. Zhang and X. Mu, *Organometallics*, 2014, **33**, 2372; X. Gu, L. Zhang, X. Zhu, S. Wang, S. Zhou, Y. Wei, G. Zhang, X. Mu, Z. Huang, D. Hong, F. Zhang, *Organometallics*, 2015, **34**, 4553; Z. Fang, Y. Wei, S. Zhou, G. Zhang, X. Zhu, L. Guo, S. Wang and X. Mu, *Dalton Trans.* 2015, **44**, 20502; X. Zhu, Y. Li, Y. Wei, S. Wang, S. Zhou and L. Zhang, *Organometallics*, 2016, **35**, 1838; X. Gu, S. Wang, Y. Wei, X. Zhu, S. Zhou, Z. Huang and X. Mu, *New J. Chem.,* 2017, **41**, 7723.
13 H. Miao, S. Wang, X. Zhu, S. Zhou, Y. Wei, Q. Yuan and X. Mu, *RSC Advances*, 2017, **7**, 42792; Z. Zhang, L. Zhang, Y. Li, L. Hong, Z. Chen and X. Zhou, *Inorg. Chem.*, 2010, **49**, 5715; G. W. Rabe, M. Zhang-Presse, F. A. Riederer and G. P. A. Yap *Inorg. Chem.*, 2002 ,**42**, 3527; H. Ding, C. Lu, X. Hu, B. Zhao, B. Wu and Y. Yao, *Synlett*, 2013, **24**, 1269; Z. Li, M. Xue, H. Yao, H. Sun, Y. Zhang and Q. Shen, *J. Organomet. Chem.*, 2012, **713**, 27; J. Qiu, M. Lu, Y. Yao, Y. Zhang, Y. Wang and Q. Shen, *Dalton Trans.*, 2013, **42**, 10179; J. Wang, T. Cai, Y. Yao, Y. Zhang and Q. Shen, *Dalton Trans.*, 2007, **36**, 5275; X. Zhu, Y. Li, Y. Wei, S. Wang, S. Zhou and L. Zhang, *Organometallics*, 2016, **35**, 1838; M. Niemeyer, *Z. Anorg. Allg. Chem*., 2002, **628**, 647; B. G. Shestakov, T. V. Mahrova, J. Larionova, J. Long, A. V. Cherkasov, G. K. Fukin, K. A. Lyssenko, W. Scherer, C. Hauf, T. V. Magdesieva, O. A. Levitskiy and A. A. Trifonov, *Organometallics*, 2015, **34**, 1177; Y. Zhou, G. P. A. Yap and D. S. Richeson, *Organometallics*, 1998, **17**, 4387; I. V. Basalov, V. Dorcet, G. K. Fukin, J.-F. Carpentier, Y. Sarazin and A. A. Trifonov, *Chem.-Eur. J.*, 2015, **21**, 6033; F. Han, Q. Teng, Y. Zhang, Y. Wang and Q. Shen, *Inorg. Chem*., 2011, **50**, 2634; G. Zi, L. Xiang and H. Song, *Organometallics*, 2008, **27**, 1242; H. C. Aspinall, D. C. Bradley, M. B. Hursthouse, K. D. Sales, N. P. C. Walker and B. Hussain, *J. Chem. Soc., Dalton Trans.*, **1989**, 623; A.-M. Dietel, C. Doring and R. Kempe, *Z. Kristallogr.-New Cryst. Struct.*, 2008, **223**, 395; X. Gu, L. Zhang, X. Zhu, S. Wang, S. Zhou, Y. Wei, G. Zhang, X. Mu, Z. Huang, D. Hong and F. Zhang, *Organometallics*, 2015, **34**, 4553; L. Cheng, Y. Feng, S. Wang, W. Luo, W. Yao, Z. Yu, X. Xi and Z. Huang, *Eur. J. Inorg. Chem.* **2007**, 1770; Z. Feng, X. Zhu, S. Wang, S. Wang, S. Zhou, Y. Wei, G. Zhang, B. Deng and X. Mu, *Inorg. Chem.*, 2013, **52**, 9549; Q. Wang, L. Xiang and G. Zi, *J. Organomet. Chem.*, 2008, **693**, 68; M. D. Fryzuk, L. Jafarpour, F. M. Kerton, J. B. Love, B. O. Patrick, S. J. Rettig, *Organometallics*, 2001, **20**, 1387; S. Sun, Q. Sun, B. Zhao, Y. Zhang, Q. Shen and Y. Yao, *Organometallics*, 2013, **32**, 1876; A. M. Dietel, C. Doring, G. Glatz, M. V. Butovskii, O. Tok, F. M. Schappacher, R. Pottgen, and R. Kempe, *Eur. J. Inorg. Chem.*, **2009**, 1051; X. Zhu, S. Zhou, S. Wang, Y. Wei, L. Zhang, F. Wang, S. Wang and Z. Feng, *Chem. Commun*., 2012, **48**, 12020; Q. Wang, L. Xiang, H. Song and G. Zi, *Inorg. Chem*., 2008, **47**, 4319; X. Zhu, J. Fan, Y. Wu, S. Wang, L. Zhang, G. Yang, Y. Wei, C. Yin, H. Zhu, S. Wu and H. Zhang, *Organometallics*, 2009, **28**, 3882; M. Lu, Y. Yao, Y. Zhang and Q. Shen, *Dalton Trans.*, 2010, **39**, 9530; Q. Li, S. Zhou, S. Wang, X. Zhu, L. Zhang, Z. Feng, L. Guo, F. Wang and Y. Wei, *Dalton Trans.*, 2013, **42**, 2861; V. Lorenz, S. Giessmann, Y. K. Gun'ko, A. K. Fischer, J. W. Gilje and F. T. Edelmann, *Angew. Chem., Int. Ed.*, 2004, **43**, 4603; R. E. Marsh, *Acta Cryst., Sect. B : Struct. Sci.,* 2009, **65**, 782; J. Qiu, M. Lu, Y. Yao, Y. Zhang, Y. Wang and Q. Shen, *Dalton Trans.*, 2013 , **42**, 10179; W. Ren, L. Chen, N. Zhao, Q. Wang, G. Hou and G. Zi, *J. Organomet. Chem.*, 2014, **758**, 65; S. Datta, M. T. Gamer and P. W. Roesky, *Organometallics*, 2008, **27**, 1207; C. Wang, L. Huang, M. Lu, B. Zhao, Y. Wang, Y. Zhang, Q. Shen and Y. Yao, *RSC Advances*, 2015, **5**, 94768; Z. Feng, Y. Wei, S. Zhou, G. Zhang, X. Zhu, L. Guo, S. Wang and X. Mu. *Dalton Trans.*, 2015, **44**, 20502; W. J. Evans, R. Anwander, U. H. Berlekamp and J. W. Ziller, *Inorg.Chem*., 1995, **34**, 3583.
14 F. Han, B. Li, Y. Zhang, Y. Wang and Q. Shen, *Organometallics*, 2010, **29**, 3467; Q. Wang, F. Zhang, H. Song and G. Zi, *J. Organomet. Chem.*, 2010, **696**, 2186; D. Qin, F. Han, Y. Yao, Y. Zhang and Q. Shen, *Dalton Trans*., 2009, **38**, 5535; I. V. Basalov, V. Dorcet, G. K. Fukin, J.-F. Carpentier, Y. Sarazin and A. A. Trifonov, *Chem.-Eur.J.,* 2015, **21**, 6033; F. Han, Q. Teng, Y. Zhang, Y. Wang and Q. Shen, *Inorg. Chem*., 2011, **50**, 2634; K. Kincaid, C. P. Gerlach, G. R. Giesbrecht, J. R. Hagadorn, G. D. Whitener, A. Shafir and J. Arnold, *Organometallics*, 1999, **18**, 5360; J. Zhang, J. Qiu, Y. Yao, Y. Zhang, Y. Wang and Q. Shen, *Organometallics*, 2012, **31**, 3138; L. Lee, D. J. Berg and G. W. Bushnell, *Inorg. Chem*., 1994, **33**, 5302.
15 F. Sinclair, J. A. Hlina, J. A. L. Wells, M. P. Shaver and P. L. Arnold, *Dalton Trans.*, 2017, **46**, 10786; L. A. Solola, A. V. Zabula, W. L. Dorfner, B. C. Manor, P. J. Carroll and E. J. Schelter, *J. Am. Chem. Soc.*, 2017, **139**, 2435; Y.-L. Wang, Y.-X. Zhou, L.-Q. Deng, Q.-S. Hu, X. Tao and Y.-Z. Shen, *J. Organomet. Chem*., 2016, **805**, 77; H. H. Karsch, G. Ferazin, H. Kooijman, O. Steigelmann, A. Schier, P. Bissinger and W. Hiller, *J. Organomet. Chem.*, 1994, **482**, 151.
16 X.-L. Wang, N. Li, A.-X. Tian, J. Ying, T.-J. Li, X.-L. Lin, J. Luan and Y. Yang, *Inorg. Chem*., 2014, **53**, 7118-7129.
17 H.-P. Xiao, J. Zhou, R.-Q. Zhao, W.-B. Zhang and Y. Huang, *Dalton Trans*., 2015, **44**, 6032; Q. Jin, J. Chen, Y. Pan, Y. Zhang and D. Jia, *J. Coord. Chem*., 2010, **63**, 1492; J.-J. Li, S. Song, D. Ma, L. Qiao, Y. Gu, F.-Y. Qian and X. Li, *Chinese J. Inorg. Chem.*, 2015, **31**, 717; C. Tang, Y. Liu, F. Wang, J. Lu, Y. Shen, Y. Zhang and D. *Jia, Inorg. Chim. Acta*, 2015, **429**, 67; Z.-P. Deng, W. Kang, L.-H. Huo, H. Zhao and S. Gao, *Dalton Trans.*, 2010, **39**, 6276; Z. Xie, Z. Liu, K. Chui, F. Xue and T. C. W. Mak, *J. Organomet. Chem.*, 1999, **588**, 78; L.-A. An, J. Zhou, H.-H. Zou, H. Xiao, R. Zhao and Q. Ding, *J. Alloys Compd*., 2017, **702**, 594; H.-T. Sheng, H. Zhou, H.-D. Guo, H.-M. Sun, Y.-M. Yao, J.-F. Wang, Y. Zhang and Q. Shen, *J. Organomet. Chem*., 2007, **692**, 1118; W. Sethi, S. Sanz, K. S. Pedersen, M. A. Srensen, G. S. Nichol, G. Lorusso, M. Evangelisti, E. K. Brechin, S. Piligkos, *Dalton Trans*., 2015, **44**, 10315.
18 D. C. Bradley, J. S. Ghotra and F. A. Hart, J. Chem. Soc., Dalton Trans., **1973**, 1021.

19 *APEX-3*, Bruker AXS, Madison, Wisconsin, USA, **2016**.
20 L. Krause, R. Herbst-Irmer, G. M. Sheldrick and D. Stalke, *J. Appl. Cryst.*, 2015, **48**, 3.
21 G. M. Sheldrick, *Acta Cryst. A*, 2015, **A71**, 3.
22 *OLEX2*, OlexSys Ltd., Durham, UK, **2017**.

Table of Contents Entry

Lanthanide complexes of 1,8-*bis*(2'-isopropyltetrazo-5'-yl)-3,6-di-tert-butylcarbazolide adopt geometries that include planar, buckled and tetrazolyl-bridged tridentate, as well as bidentate, bonding modes.